Acta Obstet Gynecol Scand 2005: 84: 716–724
Printed in UK. All rights reserved

Acta Obstetricia et Gynecologica Scandinavica

ORIGINAL ARTICLE

Magnetic resonance imaging in 300 cases of placenta accreta: surgical correlation of new findings

José M. Palacios Jaraquemada and Claudio H. Bruno

From Southern Scientific Foundation, Lomas de Zamora, Buenos Aires, and School of Medicine, University of Buenos Aires, Buenos Aires, Argentina

Acta Obstet Gynecol Scand 2005; 84: 716–724. © Acta Obstet Gynecol Scand 84 2005

Background. To establish the usefulness of placental magnetic resonance in patients with a diagnosis of placenta accreta through the correlation of diagnostic images and surgical findings.

Methods. Three hundred patients with ultrasound signs of placenta accreta were studied. In 252 patients, magnetic resonance imaging (MRI) was performed in a closed 1.5 T-resonator, and in 48 patients, open 0.23 T-set was used. T1 and T2 slices in the three planes were performed, and placental invasion was classified in depth levels and topographic areas in relation to the posterior vesical wall. The final degree of invasion was established during surgery according to clinical and anatomical criteria. The information obtained with MRI was analyzed, thus establishing its relevance to the change in surgical technique.

Results. In 286 cases, MRI provided topographic information of placental invasion, and in 90 patients, it modified invasion levels. Undiagnosed parametrium extent was determined in 11 cases, and 11 other cases were reclassified as placenta previa. Changes in conduct following MRI study included: recommendation to modify surgery date at week 35, recommendation for prophylactic ureteral catheterization, recommendation for the use of intraoperative blood salvage, possibility of approach through Pfannenstiel incision, probability of segmental myometrial approach, probability of aortic clamping, need to investigate subclinical disseminated intravascular coagulation, need of posterior pelvic dissection, and the possibility of uterine conservation.

Conclusions. Magnetic resonance imaging turned out to be essential to define the topography and area of placental invasion. New findings modified surgical tactic and technique, allowing a reduction in historical morbidity and a significant increase in conservative surgeries.

Key words: magnetic resonance imaging; placenta accreta; surgical correlation; placental invasion levels; uterine conservation

Submitted 3 August, 2004
Accepted 10 January, 2005

Placenta accreta, increta and percreta are entities of high maternal morbidity and mortality (1) and constitute in themselves several degrees of placental invasion. Abnormal placental adherence is usually associated with serious hemorrhage and myometrial damage of different size, facts that condition hysterectomy as the most frequent treatment.

Placenta previa coexisting with anterior or iterative cesarean is the main risk factor in the

Abbreviations:
DIC: disseminated intravascular coagulation; FDP: fibrinogen-degradation products; MRI: magnetic resonance imaging; pMRI: placental magnetic resonance imaging; PAD: placental adhesive disorders.

Surgical Correlation Centers: Swiss-Argentine Clinic, Mater Dei Clinic, IADT Clinic, Otamendi Clinic, CEMIC Hospital, Durand Hospital, Metropolitan Hospital, and Buenos Aires Province Hospital Network, Buenos Aires, Argentina.

development of adherent placenta (2). This association constitutes the most important clinical risk factor to suspect placental invasion. Secondly, curettage, previous uterine surgeries, and infections can be included.

Ultrasound is the first-rate method to diagnose placental invasion (3). However, it is usual to notice discrepancies between ultrasound diagnosis and surgical complexity, which make adequate therapeutic planning difficult. Therefore, it is believed that an accurate presurgery diagnosis would make it possible to minimize risks and plan a safer surgery.

Color Doppler and power Doppler were used in order to reduce the diagnostic error of conventional ultrasound (4,5). These techniques optimized the detail of the uterine–placental interface and, consequently, its diagnosis. Nevertheless, when it was necessary to characterize the lesion topography in relation to soft pelvic tissues, a placental magnetic resonance imaging (pMRI) was required (6).

Even though each type of placental adherence has a certain surgical tactic and technique, from a diagnostic point of view, we could group placenta accreta and its varieties under the label placental adhesive disorders (PAD).

Studies that have correlated pMRI and PAD are limited to small series, case presentations, retrospective analyses, or to variations in image acquisition (7–9). However, due to its excellent definition, several authors considered it necessary to make studies of statistical value to determine pMRI's real value in PAD diagnosis. It was thought that accurate diagnosis would undoubtedly imply a better surgical opportunity (10).

This study aims at establishing pMRI's usefulness in the diagnosis and treatment of PAD and at determining the correlation between diagnostic images and surgical results.

Materials and methods

Between May 1994 and May 2004, 300 pregnant women with ultrasound signs of placenta accreta were studied before MRI was performed between the 25th and 28th gestation weeks. These patients were referred from hospitals and private health care centers belonging to an estimated population area of 11 000 000 inhabitants, with an average of 40 000 living newborns per year, and a cesarean rate between 30 and 60%.

Diagnostic ultrasounds were performed at private medical institutions (79%) and at university centers (21%). All the studies were obtained and informed by well-known operators, with over 5 years experience. Ultrasound scanners with linear and sectorial 3.5 and 5 MHz transducers and also 5 and 7 MHz transvaginal transducers were employed. Ultrasound characterization for placenta accreta and its varieties was generally established according to Finberg and Williams (11) diagnostic criteria.

Ultrasound results were compared with those of pMRI in order to establish the usefulness of the new information in connection with the final surgical outcome.

In 252 patients, pMRI was performed in a Picker Edge™ 1.5 closed resonator (Picker, Cleveland, Ohio, USA). Sequences T1: SE, TE 8, TR 140, FOV 45–50, TK 8, RES 160 × 256, PS 0.602, FLIP 120°, and SAR 1.81. Breath hold and sequences T2: FSE 32; TE 168; TR 3500; FOV 28; THCK 8; GAP 1.5; RES 192 × 256; PS 1.328; FLIP 90; NSA 1; SAR 2.25. In the remaining 48 patients, a 0.23 T open Picker Outlook Proview™ resonator was used (Marconi, Vantaa, Finland) HOLD FE-92/6.0, FA 90°, SI. Thk/sep: 10/11 mm, FOV 200 × 256, Phase enc: HOR, ETL 1. All patients ingested 750 ml of water 45 min before the study, and slices in the three spatial planes were used. All pMRI were performed between the 30th and the 33rd gestation weeks. The examination time was nearly 30 min and almost always well tolerated, and approximately only 12% of the patients suffered from claustrophobia and requested the open resonator.

Sagittal images obtained through pMRI allowed the division of anterior placental invasion into two sectors (12). Both were delimited by a plane perpendicular to the upper bladder axis, and the uterine sector bordering con the upper posterior bladder wall is called S1, and the uterine sector adjacent to the lower posterior wall, S2 (Figs 1 and 2). The levels of placental invasion determined by pMRI were labeled: 0, for absence of invasion; A, for partial myometrial invasion; B, for total

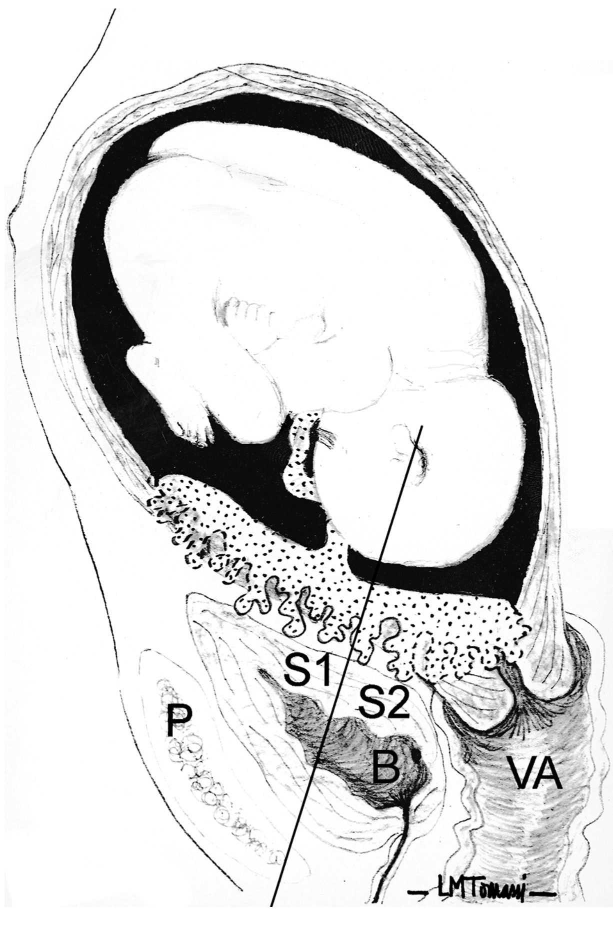

Fig. 1. Sagittal cut of pelvis. The division plane can be seen in sectors S1 (upper uterine segment) and S2 (lower uterine segment). P, pubis; VA, vagina; B, bladder.

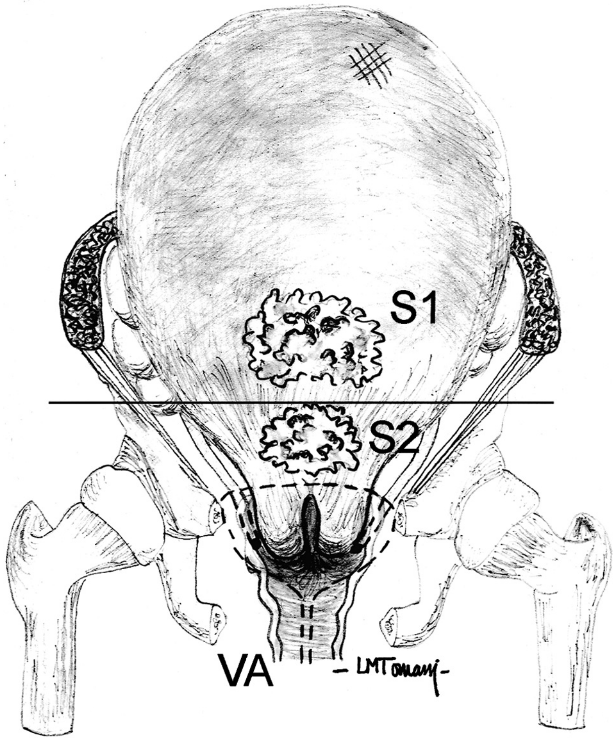

Fig. 2. Frontal view of pelvis. Both types of anterior invasion S1 (upper uterine segment) and S2 (lower uterine segment) can be observed. VA, Vagina.

myometrial invasion; and C, for invasions that involved the whole of the myometrium and that included one or both parametriums (seen in the pMRI's coronal and axial slices). For the case of combined S1 and S2 invasions, groups were formed according to the highest percentage of invasion.

The final degree of placental penetration and its specific topography were established in the operating room according to clinical and anatomical criteria. With that purpose, placenta accreta was defined as that which adhered itself firmly to the endometrium, and that which, when detached, showed non-self-controlled bleeding, placenta increta as that which required curettage to remove invasive tissue deeply implanted in the myometrium, and placenta percreta as that invasion which involved all uterine layers, being able to exceed the uterus and invade neighboring organs.

Information that had not been provided by previous studies was considered new, and data which modified surgical tactic or technique were considered relevant information.

pMRI findings were compared with final surgical results. With that aim, specific surgery was performed following a pre-established protocol (13). There, laparotomy and myometrial approach was considered according to the area and depth of placental invasion, being fit for uterine reconstructive surgery those placental invasions which did not affect more than 50% of uterine axial circumference. The surgical protocol included precise parameters for vascular control which, according to the case, would be performed in the pelvic vessels (parametrium) or in the infrarenal abdominal aorta. Once fetal extraction and pelvic fascial dissection were concluded, myometrium and vesical reconstruction was made according to specific technique or to hysterectomy when necessary.

Tests of statistical significance Chi-square were performed, between S1 and S2 levels established by pMRI topographic classification. Parameters of comparison included the possibility of uterine conservation, hysterectomy, and the volume of transfused blood.

Results

Mother's age ranged between 16 and 46 years. Patients reported 87 miscarriages, 61 of which where solved without curettage. Myomectomy background was recorded in 29 patients, 14 cases belonging to corporal myomas and 8 to fundal myomas. In the seven remaining cases, their exact location could not be defined due to lack of reliable documentation.

Placental implantation corresponded to 206 previous locations, 69 anterior ones, and 25 to lower anterior ones.

Analysis of the relation between the number of cesarean and invasion levels can be examined in Table I. The most frequent invasion was the A type with 72.88%, and B and C invasions were for one to two cesareans in 5.42% and for three or more in 19%, respectively. C invasions (parametrium invasions) were evidenced only through pMRI. Ultrasound type, its diagnosis, and also the new information obtained by pMRI can be seen in Table II.

pMRI modified the interpretation of invasion degree in 90 patients (30%), and classified invasion topography in 286 patients (95.33%). In 14 cases, invasion anatomy through studies with incomplete series could not be defined, caused by fetal movement or intolerance to study.

Surgical results were closely related to the kind and level of invasion evidenced through pMRI (Table III). Changes in conduct secondary to pMRI study included: surgery rescheduling at week 35 (68 cases), ureteral catheterization (11 cases), indication of intraoperative blood salvage (43 cases), presence of specialists (43 cases), possibility of Pfannenstiel incision (19 cases), segmental myometrial approach (34 cases), aortic vascular control (22 cases), detection of subclinical disseminated intravascular coagulation (21 cases), posterior pelvic dissection (15 cases), and possibility of uterine conservation (236 cases).

In 281 patients (93.66%), direct and personal correlation was made between images and surgical findings. In the 19 remaining cases, surgical correlation was performed by others.

Table I. Previous cesarean and degree of invasion (regardless of pMRI classification)

pMRI	0	A	B	C
One cesarean	5	22	3	1
Two cesarean	6	38	9	3
Three cesarean	0	73	16	2
Four or more	0	82	27	13
Total 300	11	215	55	19

pMRI, placental magnetic resonance imaging. 0, no invasion; A, partial invasion; B, total invasion; C, parametrial invasion.

Table II. Previous diagnosis and pMRI new information

	AB US	TV US	DP US	US diagnosis	pMRI NF	
					Degree	S1/S2 location
Group 1 ($n = 38$)	38	0	0	Placenta accreta: 26 Placenta increta: 12	Invasion 0: 7 Invasion B: 11 Invasion C: 3	S1: 20 S2: 11
Group 2 ($n = 134$)	134	43	0	Placenta accreta: 102 Placenta increta: 30 Placenta percreta: 2	Invasion 0: 4 Invasion B: 17 Invasion C: 3	S1: 79 S2: 47
Group 3 ($n = 128$)	128	102	97	Placenta accreta: 88 Placenta increta: 38 Placenta percreta: 2	Invasion B: 40 Invasion C: 5	S1: 82 S2: 45
Total	300	145	97	300	NF: 90 (30%)	NF: 284 (94.66%)

AB US, abdominal ultrasound; D US: Doppler ultrasound; pMRI, placental magnetic resonance imaging; NF, new findings; TV US, transvaginal ultrasound. 0, no invasion; A, partial invasion; B, total invasion; C, parametrial invasion. Group 1, AB US; group 2, AB US + TV US; group 3, AB US + TV US + Doppler.

Total hysterectomy was indicated in 30 patients, out of which, 22 cases corresponded to massive myometrial destruction (over 50% of uterine axial circumference). In the other eight cases, hysterectomy was advised because of coagulopathy.

pMRI accurately characterized the level and topography of invasion in 97.66% of the cases. Four false positives for placenta percreta (1.33%) and three false negatives for placental invasion (1%) were recorded.

Because the uterine conservation was performed in most cases, the histology of placental invasion was enable only in 30 cases, 20 of them were placenta percretas (B and C invasion), and the other 10 were classified as placenta accretas (A invasion).

Chi-square test-established significant differences ($P < 0.001$) between S1 and S2 invasion levels (pMRI) related to the possibility of uterine conservation, hysterectomy, and transfused blood volume.

Discussion

It is usual to observe discrepancies among the ultrasound report, histology, and surgical complexity of PAD (14,15). Repetition of these differences would imply the usefulness of replacing the morphological classification with a topographic one. This change would allow the analysis of diagnostic information with the main aim of planning the surgery.

The division into S1 and S2 topographic areas is directly related to the degree of local irrigation (16). Sector S1 is irrigated by the uterine and upper vesical arteries, vessels which are generally of easy access and which promote quick hemostasis. However, sector S2 has anastomotic irrigation and originated in multiple pedicles (Fig. 3). The visceral intersection formed among the vesical trigonum, the uterine cervix, and the vagina is irrigated by deeply located vessels (pelvic subperitoneal), a fact which significantly increases S2's surgical complexity and the possibility of hemorrhage.

S2 B and C invasions imply a higher probability of using specific procedures, such as aortic clamping (17) or posterior ureteral dissection that is mainly due to the difficulty to perform a bloodless dissection or at least controlled within a vascular magma located deeply inside the pelvis. Besides, and because of, its higher hemorrhagic probability, it is convenient to use intraoperative blood salvage in this kind of invasions. This

Table III. Analysis by localization and outcome (pMRI classification)

	0	A	B	C
S1		136	49	5
UC (%)		136 (100)	47 (95.9)	3 (60)
TAH (%)		0 (0)	2 (4.1)	2 (40)
TR		0–1 U (0.25 median)	1–3 U (1.79 median)	1–4 U (2.2 median)
S2		70	23	6
UC (%)		60 (85.7)	12 (52.17)	1 (16.6)
TAH (%)		10 (14.3)	11 (47.83)	5 (83.4)
TR		2–5 U (3.2 median)	5–10 U (6.9 median)	3–7 U (5.16 median)
Total ($n = 300$)	11 (UC 100%)	206	72	11

TAH, total abdominal hysterectomy; UC, uterine conservation. 0, no invasion; A, partial invasion; B, total invasion; C, parametrial invasion; TR, transfusions.

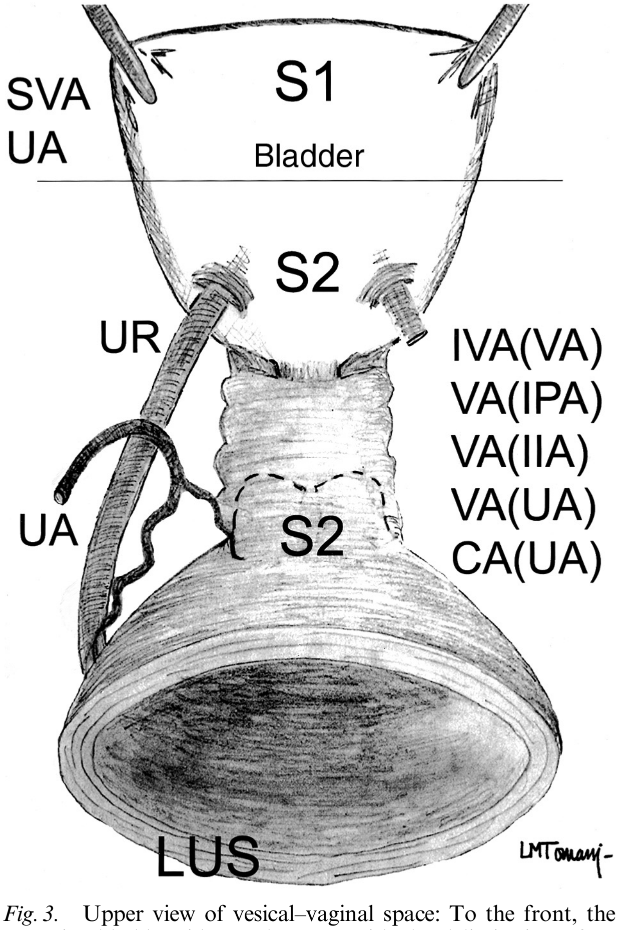

Fig. 3. Upper view of vesical–vaginal space: To the front, the posterior bladder side can be seen, with the delimitation of S1 and S2 sectors. Behind, the homonymous sector corresponding to S2 (lower uterine segment, cervix, and vagina) can be observed. S1 pedicles: SVA, superior vesical artery; UA, uterine artery. S2 pedicles: IVA, inferior vesical artery; VA: vaginal artery from (1) IPA, inferior pudendal artery; (2) IIA: iliac internal artery; (3) UA, uterine artery. CA, cervical artery from the uterine artery; LUS: lower uterine segment; UR: Ureter.

recommendation may be deemed invaluable when availability of the specific group is limited. The sum of particular difficulties and the reduced circumference area cause most S2 B and C invasions to usually require resection procedures and a higher number of transfusions.

It has been observed that S2 B and C invasions may be accompanied by subclinical hemostatic alterations, such as fibrinogen consumption, high levels of fibrinogen-degradation product, or a combination of both. Even though presurgery incidence of these disorders is low (10–15%), prediction of complications (hematologist and resources in the operating room) has allowed a significant decrease of surgical morbidity (personal unpublished data).

Specific topographic knowledge of placental invasion (S1 A, B and S2 A) provides the possibility of performing a segmental approach and also of performing a Pfannenstiel incision using predetermined dissecting vascular control techniques. In this respect, neither ultrasound nor Doppler could delimit the invasion area per regions or indicate lines for a differential approach.

Presurgery localization of B and C invasions (percreta and parametrial invasions) turned out to be vital to plan surgery on week 35. This fact is usually essential, because after that date, a higher number of complications have been proved (18).

Axial and coronal slices obtained by pMRI have made it possible to evidence parametrial invasion in 100% of the cases. This finding, so far unique for pMRI, would make it possible in S2 B and C lesions to suggest the placement of a urinary catheter in order to prevent possible ureteral injuries during deep pelvic dissection (19), which is, topographically, a hard-access area and noticeably irrigated (Fig. 4). For this reason, pMRI constitutes a best topographic study for the surgical planning of PAD (20).

Invasion topography (S1 and S2) showed significant differences in both groups in relation to the possibility of uterine conservation, hysterectomy, and hematological resources. Characterization of the degree of invasion was particularly efficient when the study was associated to topographic parameters. Changes in surgical tactic and technique were a direct consequence of the additional and suitable information provided by pMRI.

Despite the evidence collected, pMRI in itself should neither establish nor determine unavoidable therapeutic techniques. On the contrary, it is a study that would allow the planning of options and resources to reduce or avoid PAD's inherent complications. Due to the current impossibility of setting a diagnostic 'gold standard' for PAD, it is advisable that the last therapeutic decision should always be made in the operating room, according to an actual estimation of the damage, to vascular

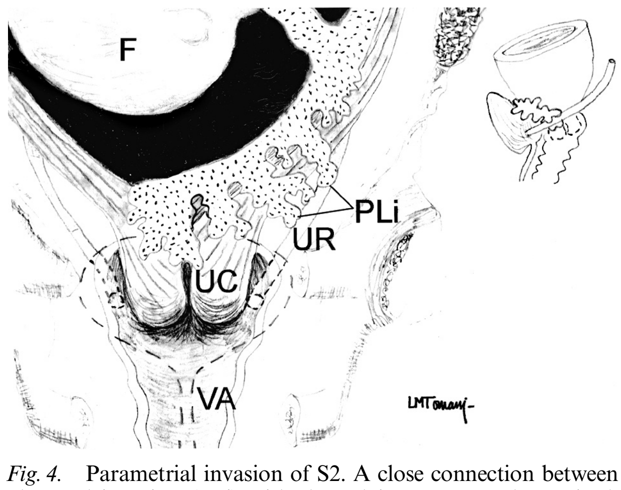

Fig. 4. Parametrial invasion of S2. A close connection between placental invasion (PLi) with the pelvic ureter can be noticed. UR,ureter; F, fetus; UC, uterine cervix; VA: vagina.

control probabilities, and to the ability to perform adequate tissue reconstruction.

As 30% of the patients have been relocated to 0, B or C types, it is advisable not to establish definitive actions before the topographic study (pMRI) has been completed and the final diagnosis through direct inspection has been verified.

The number of false positives observed in the series was low (four cases). Diagnostic error was a result of noticing thick vessels in the vesical–segmental interface, which gave the diagnostic impression of placenta percreta (21). In these cases, the absence of clinical background cast doubt on the veracity of the diagnosis by pMRI, and the four cases were approached through a Pfannenstiel incision. However, the identification of the vascular pattern mentioned enabled a conditioned wide exposition and ligature of the intramyometrial vessels (Fig. 5), a tactic that avoided an additional hemorrhage during hysterectomy. The three false negatives were due to studies with incomplete sequences, generally caused by intolerance to the study or by fetal movement. In these cases, and despite the fact that we could not define the morphological characteristics with certainty, the patients were operated on as B invasions (classical percretas) due to their clinical background.

From a technical point of view, slice thickness and the use of image filters can also be regarded as causes of pMRI's diagnostic error. In our teams, the use of slice thickeners under 7 mm caused overgaining (false positives), and interfered in the valuation of the vesical–placental interface. In contrast, the use of high- and mid-image filters eliminates the faint image produced by the neoformation vessels (false negatives), and it leads to underestimation of the actual degree of invasion.

pMRI has proved to be innocuous during pregnancy (22,23), and so far, its indications in PAD cases used to be limited to cases with a diagnostic doubt or with the suspicion of posterior placental invasion (24). This study would allow the recommendation of pMRI in patients with a diagnosis of placenta increta or percreta, especially if they experience low pelvic pain or irradiated to the back, both usual symptoms of C invasions. Besides, pMRI is recommended in patients with PAD and who are eager to keep the uterus, or interested in a future pregnancy. In these patients, sectional lesion anatomy is particularly useful to plan the approach (25), vascular control, and possible uterine reconstruction.

As other authors have already stated, a precise diagnosis has improved the actual possibilities to treat PAD. Non-gestational functions of the uterus are beginning to be revealed, and they appear to be remarkable (26,27). Therefore, we consider it useful to have any resource that can make uterine conservation easy or that can promote it. In this respect, the topographic characterization performed by pMRI, together with the use of specific surgical techniques, has made it possible to achieve a high rate of uterine conservation with minimal complications.

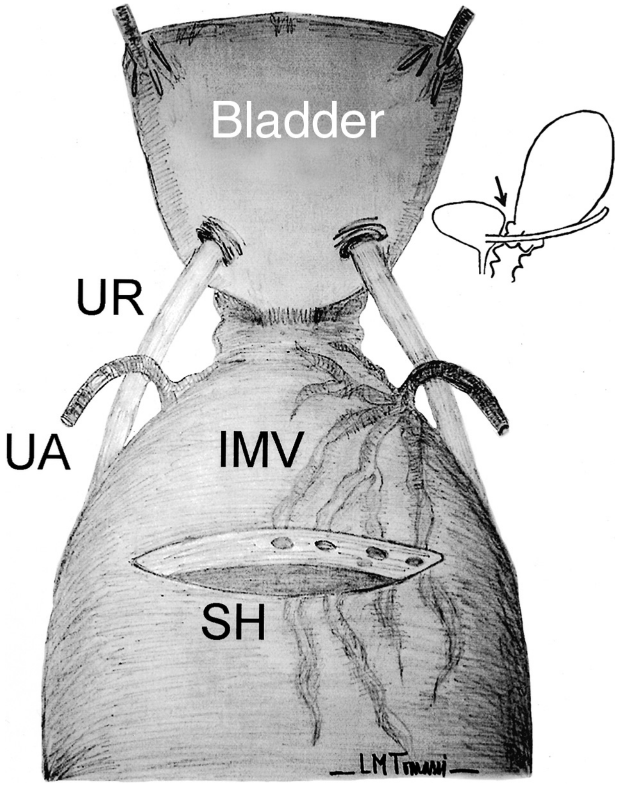

Fig. 5. Upper view of the vesical–vaginal space: thick intramyometrial vessels (IMV) in the thickness of the uterine segment can be observed, simulating neo-formation vessels of placenta percreta. SH, segmental hysterotomy; UR, ureter; UA, uterine artery.

Image gallery

A 1: Axial slice; A type C (parametrial) placental invasion can be identified. Behind and on the right, thick neo-formation vessels (NFV) can be identified marked with an asterisk.

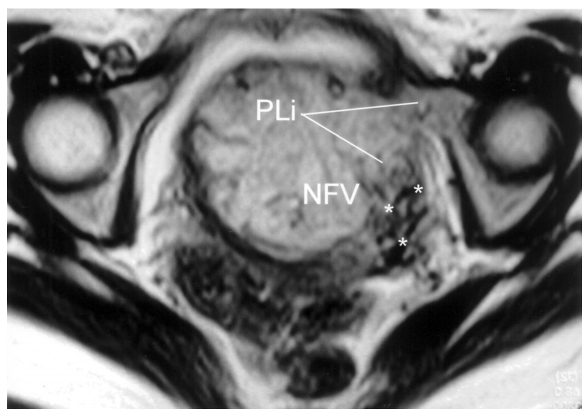

A 2: Axial slice; placental invasion (PLi) of the posterior bladder region.

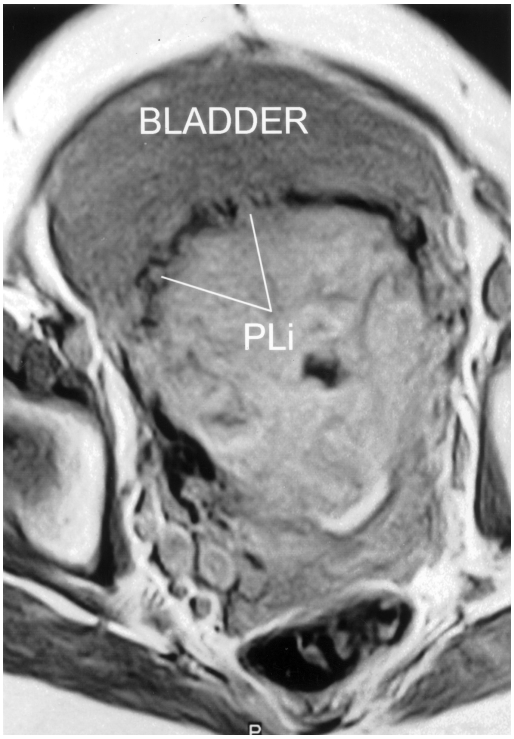

A 3: Axial slice; retrovesical rupture of the uterine segment. Placenta has invaded (PLi) the vesical seromuscular and protrudes into the vesical mucosa. The absence of neo-formation vessels is an indicator of a good surgical prognosis.

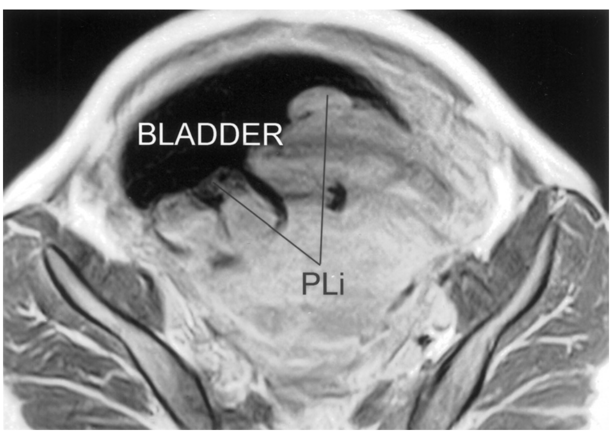

1 C: Coronal slice; in the vesical–placental interface areas of placental invasion (PLi) can be observed. On the picture's right margin, images of flow vacuum can be identified (with an asterisk) due to the neo-formation vessels (NFV).

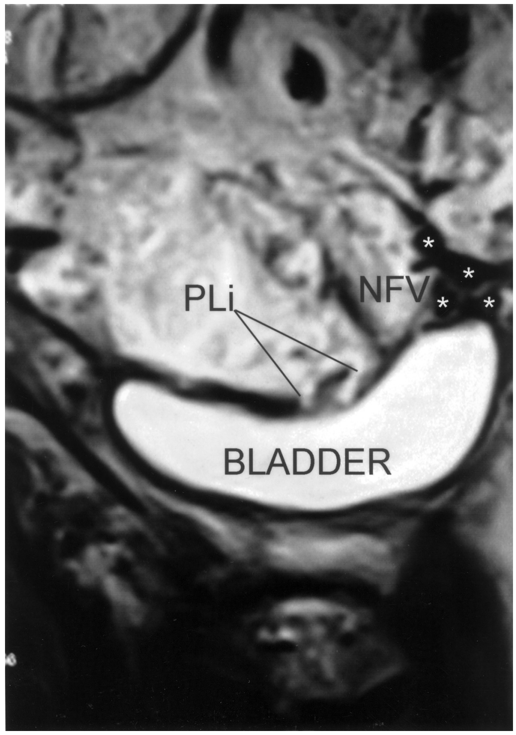

2 C: Coronal slice; 19-week pregnancy, fetus (F). A type C placental invasion (PLi) can be seen, which infiltrates into all uterine layers and reaches the pelvic lateral wall.

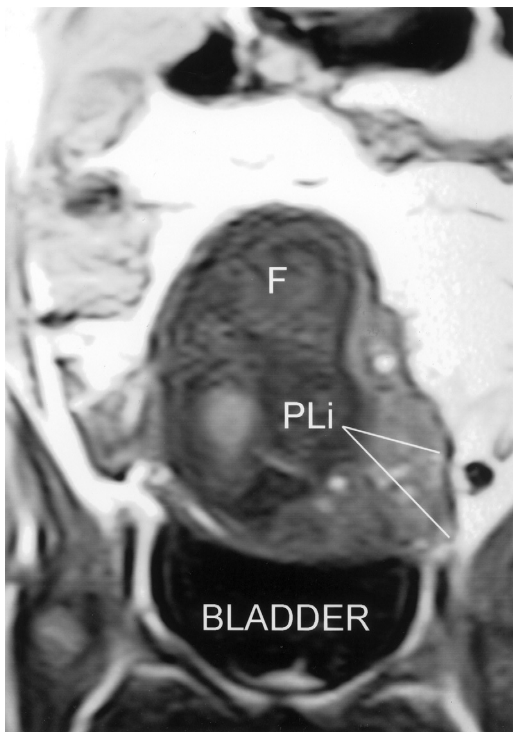

3 C: Coronal slice; massive invasion of bladder and of both parametriums (PLi). Images of flow vacuum characteristic of neo-formation vessels (NFV) have been marked with an asterisk. (B) Bladder.

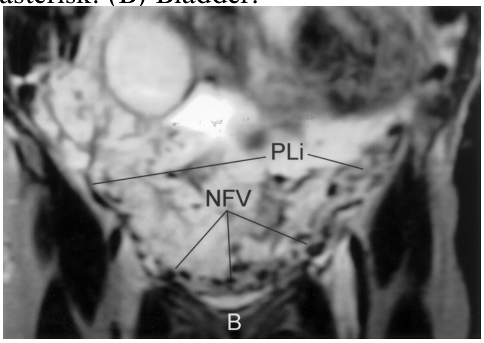

4 C: Coronal slice; the way the placenta invades (PLi) and protrudes into the bladder (B) can be observed here. Fetal head (F).

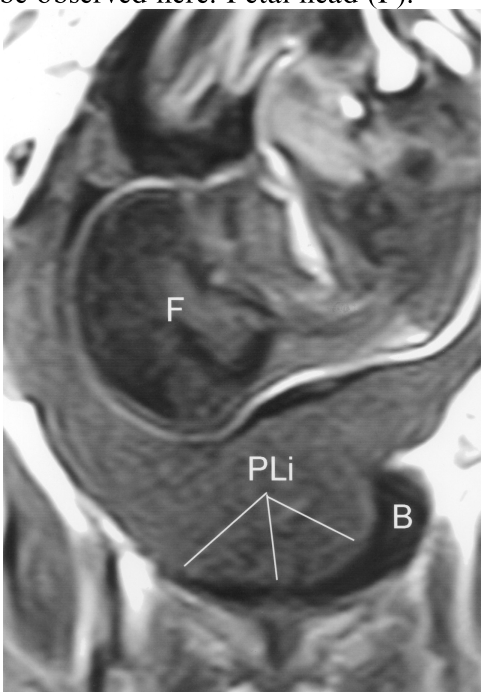

4 D: Coronal slice; on the left side (with an asterisk), vascular infiltration of the vesical seromuscular can be observed. PLi, placental invasion; NFV, neo-formation vessels.

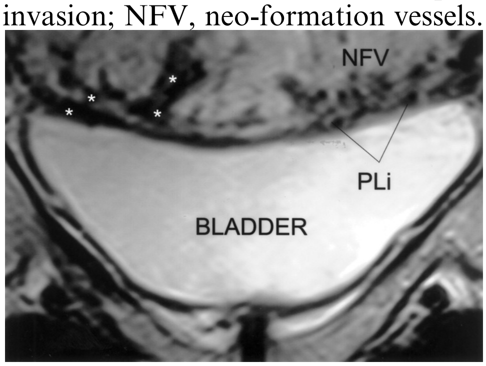

S 1: Sagittal slice; vesical delimitation of S1 and S2 invasion areas. NFV, neo-formation vessels.

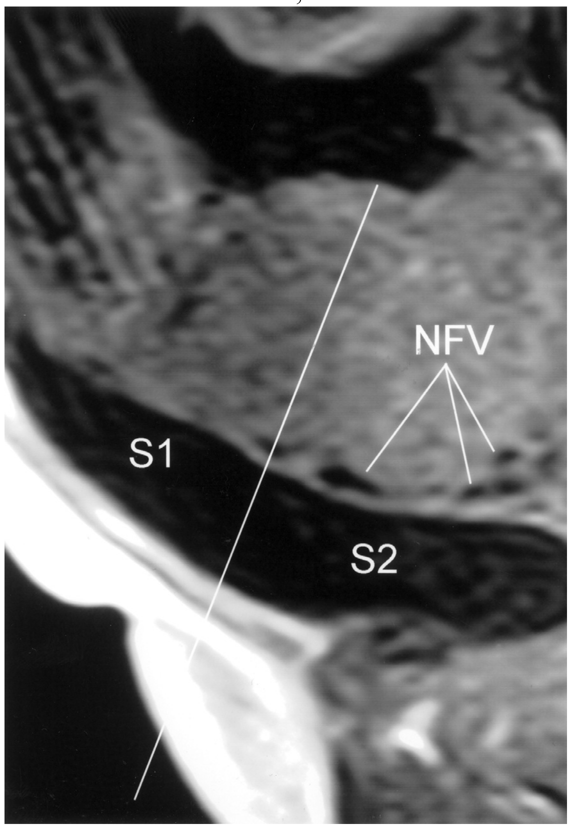

S 2: Sagittal slice; placental invasion of all the posterior side of the bladder (PLi), B, bladder.

S 3: Sagittal slice; placental invasion (PLi) in different sectors of the vesical posterior wall can be noticed.

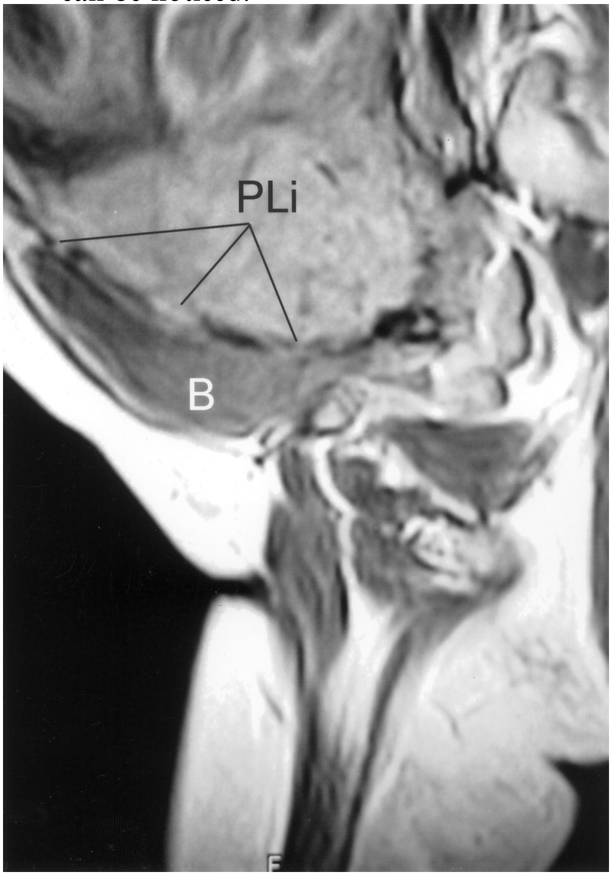

Acknowledgments

We thank Dr Otaño L. and García Mónaco R. for their critical review of the manuscript. Also, we would also like to offer special thanks to Sarroca D., and also to Zangari P. for her accurate and careful assistance to the patients, and to the obstetricians who collaborated with the surgical correlation score.

References

1. Breen JL, Neubecker RL. Placenta accreta. ACOG Committee Opinion No 266. American College of Obstetrician and Gynecologists. Obstet Gynecol 2002; 99: 169–70.
2. Miller DA, Chollet JA, Goodwin TM. Clinical risk factors for placenta previa – Placenta accreta. Am J Obstet Gynecol 1997; 177: 210–4.
3. Hoffman-Tretin J, Koenigsberg M, Rabin A, Anyaegbunam A. Placenta accreta, additional sonographic observations. J Ultrasound Med 1992; 34: 29–34.
4. Twickler DM, Lucas MJ, Brown Balis A, Santos-Ramos R, Martin L, Malone S et al. Color flow mapping for myometrial invasion in women with a prior caesarean delivery. J Matern Fet Med 2000; 9: 330–5.
5. Lerner JP, Deane S, Timor-Tritsch IE. Characterization of placenta accreta using transvaginal sonography and color Doppler imaging. Ultrasound Obstet Gynecol 1995; 5: 198–201.
6. Thorp JM, Councell RB, Sandridge DA, Iest HH. Antepartum diagnosis of placenta previa percreta by magnetic resonance imaging. Obstet Gynecol 1992; 80: 506–8.
7. Fejgin MD, Rosen DJ, Goldberg SB, Beyth Y. Ultrasonic and magnetic resonance imaging diagnosis of placenta accreta managed conservatively. J Perinat Med 1993; 21: 165–8.
8. Taryn PTH, Li KCP. Placenta accreta: MRI antenatal diagnosis and surgical correlation. JMRI 1998; 8: 748–50.
9. Thorp JM Jr, Wells SR, Wiest HH, Jeffies L, Lyles E. First trimester diagnosis of placenta previa percreta by magnetic resonance imaging. Am J Obstet Gynecol 1998 March; 178: 616–8.
10. Kirkinen P, Helin-Martikainen HL, Vanninen R, Partanen K. Placenta accreta: imaging by gray-scale and contrasted-enhanced color Doppler sonography and magnetic resonance imaging. J Clin Ultrasound 1998; 26: 90–4.
11. Finberg HJ, Williams JW. Placenta accreta: prospective sonographic diagnosis in patients with placenta previa and prior cesarean delivery. J Ultrasound Med 1992; 11: 333–43.
12. Palacios Jaraquemada JM, Pesaresi M, Nassif JC, Hermosid S. Anterior placenta percreta: Surgical approach, hemostasis and uterine repair. Acta Obstet Gynecol Scand 2004; 83: 738–44.
13. Palacios Jaraquemada JM, Pesaresi M, Hermosid S, Nassif JC, Zlatkes R et al. Conservative treatment in placenta accreta and percreta. Available at: http://www.obgyn.net/us/us.asp?page=/us/present/0701/jaraquemada (retrieved on July25, 2001).
14. Gielchinsky Y, Rojansky N, Fasouliotis SJ, Ezra Y. Placenta accreta – summary of 10 years: a survey of 310 cases. Placenta 2000; 23: 210–4.
15. Irving FC, Hertig AT. A study of placenta accreta. Surg Gynecol Obstet 1937; 64: 178–200.
16. Palacios Jaraquemada JM. Anatomy study of arterial circulation of the pelvis. Surgical considerations. Doctorate Thesis, School of Medicine, University of Buenos Aires 1997 (in Spanish).
17. Palacios Jaraquemada JM, Pesaresi M, Nassif JC, Hermosid S, Sarto A et al. Aortic cross-clamping in obstetrics. Available at http://www.obgyn.net/displayarticle.asp?page=/english/pubs/features/pov-aortic_cross (retrieved on October3, 2001).
18. O'Brien JM, Barton JR, Donaldson ES. The management of placenta percreta: conservative and operative strategies. Am J Obstet Gynecol 1996; 175: 1632–8.
19. Chan JK, Morrow J, Manetta A. Prevention of ureteral injuries in gynecologic surgery. Am J Obstet Gynecol 2003; 188: 1273–7.
20. Maldjian C, Adam R, Pelosi M, Pelosi M III, Rudelli RD, Maldjian J. MRI appearance of placenta percreta and placenta accreta. J Magn Reson Imaging 1999; 17: 965–71.
21. Russ PD, Tomaszewski G, Coffin C. Pelvic varices mimicking placenta percreta at sonography. SDMS 2000; 16: 183–90.
22. Kanal E. Pregnancy and the safety of magnetic resonance imaging. Magn Reson Imaging Clin N Am 1994; 2: 309–19.
23. Colletti PM, Sylvestre PB. Magnetic resonance imaging in pregnancy. Magn Reson Imaging Clin N Am 1994; 2: 291–307.
24. Levine D, Hulka CA, Ludmir J, Li W, Edelman RR. Placenta accreta: evaluation with color Doppler US, Power Doppler US, and MR imaging. Radiology 1997; 205: 773–6.
25. Pelosi MA III, Pelosi MA. Modified cesarean hysterectomy for placenta previa percreta with bladder invasion: retrovesical lower uterine segment bypass. Obstet Gynecol 1999; 93: 830–3.
26. Cheng S, Sievänen H, Heinonen A, Uusi-Rasi K, Carbone L, Tylavsky F et al. Does hysterectomy with ovarian conservation affect bone metabolism and density? J Bone Miner Metab 2003; 21: 12–6.
27. Luoto R, Grenman S, Salonen S, StudMed Pukkala E. Increased risk of thyroid cancer among women with hysterectomies. Am J Obstet Gynecol 2003; 188: 45–8.

Address for correspondence:
José Miguel Palacios Jaraquemada
Av. Corrientes 5087
4° A, C1414AJD
Ciudad Autónoma de Buenos Aires
Argentina
e-mail: jpalacios@ciudad.com.ar